AN AUGMENTED STATE VECTOR APPROACH TO GPS-BASED LOCALIZATION

Francesco Capezio, Antonio Sgorbissa and Renato Zaccaria
Laboratorium D.I.S.T. – University of Genova

Keywords: Mobile Robotics; Localization; State Estimation.

Abstract: The ANSER project (Airport Night Surveillance Expert Robot) is described, exploiting a mobile robot for autonomous surveillance in civilian airports and similar wide outdoor areas. The paper focuses on the localization subsystem of the patrolling robot, composed of a non-differential GPS unit and a laser rangefinder for map-based localization (inertial sensors are absent). Moreover, it shows that an augmented state vector approach and an Extended Kalman filter can be successfully employed to estimate the colored components in GPS noise, thus getting closer to the conditions for the EKF to be applicable.

1 INTRODUCTION

The work described in this paper is part of the ANSER[1] project, an ongoing project for autonomous surveillance in civilian airports and similar wide outdoor areas[2]. Within this framework, a system composed of two parts is foreseen: a mobile autonomous robot (also referred to as UGV – Unmanned Ground Vehicle), whose sensors and actuators have been especially crafted to successfully perform night patrols, and a fixed supervision station, which is under direct control of a human supervisor. The main surveillance task is to detect differences between perceived and expected environmental conditions; in particular to verify the state of doors and barriers, to verify the presence of allowed/non allowed persons in the current area, and to identify unexpected objects. In ANSER, this is done through the combination of a laser rangefinder and an on-board panning video camera, and it obviously requires a sufficient accuracy in self-localization to be able to recognize "what is normal" and "what is not" in a given area. A first system prototype is currently being tested at the Villanova d'Albenga Airport (Figure 6), where it is asked to patrol a wide outdoor area and the indoor Airport Terminal.

In the last years several autonomous surveillance systems based on a mobile platform have been presented.

A very interesting example in this sense is the MDARS project, a joint USA Army-Navy development effort (Heath-Pastore, *et al.*, 1999). The MDARS goal is to provide multiple mobile platforms that perform random patrols within assigned areas of warehouses and storage sites, both indoor and in semi-structured outdoor environments, such as storage yards, dock facilities, and airfields. MDARS-E apparently meets the requirements of the ANSER domain. However, it is immediate to notice that high performance are obtained by over equipping the system with a huge set of different sensorial devices and – consequently – providing adequate onboard computing power to process the huge amount of available data. For example, the localization and navigation subsystem of MDARS-E requires the joint use of a differential GPS, a fiber-optic gyro and the recognition of retroreflective landmarks via a laser-based proximity sensor.

In (Saptharishi, *et al.*, 2002) a network of mobile all-terrain vehicles and stationary sentries are exploited in an autonomous surveillance and reconnaissance system. The vehicles are equipped with video cameras, and are able to detect moving objects, classify them using a differential learning algorithm, and track their motion. Each robot relies for localization on a Differential GPS and an IMU (Inertial Measurement Unit); a PC/104 for the

[1] ANSER is an acronym for Airport Night Surveillance Expert Robot, and the Latin name for "goose" (referring to the Capitoline Geese which –according to tradition - neutralized a nighttime attack by the Gauls during the siege of Rome).

[2] Funded by the Parco Scientifico Tecnologico della Liguria (PSTL), www.pstliguria.it.

Capezio F., Sgorbissa A. and Zaccaria R. (2007).
AN AUGMENTED STATE VECTOR APPROACH TO GPS-BASED LOCALIZATION.
In *Proceedings of the Fourth International Conference on Informatics in Control, Automation and Robotics*, pages 252-258
DOI: 10.5220/0001626302520258

locomotion task, and three networked PCs for planning, perception and communication are required.

In (Vidal, *et al.*, 2002) a team of UAVs (Unmanned Arial Vehicle) and UGVs pursue a second team of evaders adopting a probabilistic game theory approach (pursuit-evasion is a classical problem that had been deeply investigated (Volkan, *et al.*, 2005)). Also in this case, the robots need enough computational power to manage a Differential GPS receiver, an IMU, video cameras and a color-tracking vision system.

In (Rybski,*et al.*, 2002) a multirobot surveillance system is presented. A group of miniature robots (Scouts) accomplishes simple surveillance task using an on-board video camera. Because of limitations on the space and power supply available on-board, Scouts rely on remote computers that manage all the resources, compute the decision processes, and finally provide them with action control commands.

As one could expect, autonomous navigation and self-localization capabilities are a fundamental prerequisites in all these systems. This is the reason why, starting from a minimal configuration in which self-localization relies on an Inertial Measurement Unit (IMU) and a Carrier Phase, Differential GPS receiver (CP-DGPS) – see for example (Panzieri, *et al.*, 2002; Schönberg, *et al.*, 1995; Dissanayake, *et al.* 2001; Farrell, *et al.*, 2000) -, a very common approach is to equip the mobile platform with a large set of sensors (video cameras, PIR sensor, RFID sensor, sonar, laser range finders etc.), thus consequently requiring a high computational power and complex data filtering techniques.

In partial contrast with this "over equipping" philosophy, the ANSER self-localization sub-system relies only on a standard (non-differential) GPS unit, and on a laser rangefinder. Unfortunately, GPS data are known to be affected by low-frequency errors that cannot be modeled as zero mean, Additive White Gaussian Noise (AWGN), thus making simple state estimation approaches (e.g., Kalman Filter) unfeasible (Sasiadek, and Wang, 2003). As a main contribution, this work proposes to estimate the low-frequency components of GPS noise through an augmented state vector approach, similar to (Farrell, *et al.*, 2000) (Martinelli, 2002). The paper shows that, by combining laser-based localization and GPS measurement, it is possible to estimate both the robot's position and the non-AWG components of GPS noise.

Section II briefly describes the localization techniques adopted; Section III theoretically investigates the properties of the approach, and carries out an observability analysis; Section IV presents experimental results obtained so far with a realistic simulator, and in a field set-up at the Villanova d'Albenga Airport. Conclusions follow.

2 GPS- AND LASER-BASED SELF-LOCALIZATION

2.1 Gps Based Localization

A single non-differential GPS receiver provides the mobile robot with absolute position measurements, that can be employed to correct the estimate provided by odometry. Unfortunately, the measurement process is corrupted by different error sources, which are consequence of the receiver and the satellites clock bias, the atmospheric delay, the multi-path effect, etc. (Farrell, *et al.*, 2000). The union of these errors is known as Common Mode Error, and it introduces into the GPS measure a greatly colored noise with a significant low-frequency component. Approximately, this can be modeled as a non-zero mean value in GPS errors that varies slowly in time (in the following, it will be referred to as a "bias" in GPS measurements).

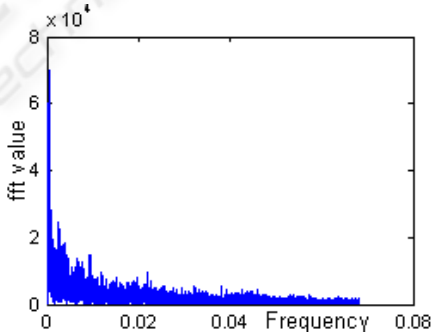

Figure 1: FFT of GPS latitude data.

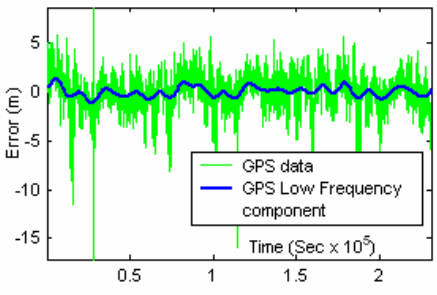

Figure 2: The estimated GPS bias.

The analysis of longitude and latitude data collected at a fixed location during 24 hours shows this effect: by considering the Fast Fourier Transform (FFT) of GPS longitude and latitude data (the latter is shown in Figure 1), low-frequency components can be noticed, corresponding to slow variation of the signal in time. By estimating this bias in GPS measurements, one can expect that – at least in theory – the precision of GPS data should improve, therefore making localization more accurate. The low-frequency component of latitude error is shown separately in Figure 2.

To estimate the bias, an augmented state vector **x** is defined; **x** comprises both (x, y, θ) components of the robot's position, and the (x_{GPS} , y_{GPS}) components of the low-frequency bias in GPS measurements. Notice that, by separating the colored components from Additive White Gaussian components of GPS noise, the system gets closer to the conditions for the Extended Kalman Filter to be applicable. When new measurements are available (i.e., both GPS data and the features detected by a laser rangefinders), the full state vector can be estimated through observations.

2.2 Laser Based Localization

When moving indoor, the robot is provided with an a-priori map of the environment; the laser-based localization subsystem simply updates the position by comparing this map with the features detected by the laser rangefinder.

In particular, (Capezio, *et al.*, 2006) describes in details how segment-like features are extracted from raw data and compared with the a-priori model: 1) line extraction produces a set of lines $\{ l_j \}$; 2) the Mahalanobis distance associated to each couple of line (l_j, m_i) is computed (where $\{ m_i \}$ is a set of oriented segment lines that define the a-priori map); 3) for each l_j, the line m_i for which such distance is minimum is selected and fed to the EKF.

When moving outdoor, lines in the a-priori map correspond to the external walls of buildings. Obviously, a smaller number of features is available outdoor, since the robot mostly traverses areas where no buildings are present at all (especially in the Airport scenario). However, when features are available, they are sufficient to estimate the full state vector, and – under some assumptions – the estimate stays valid even when the laser cannot provide any further information.

3 SYSTEM ARCHITECTURE

As anticipated, the proposed approach relies on the idea of "guessing" the bias that affects GPS measurements at a given time, by including it in the state to be estimated. The resulting augmented state vector is shown in Equation 1.

$$\mathbf{x}^T = \begin{bmatrix} x & y & \theta & x_{GPS} & y_{GPS} \end{bmatrix} \quad (1)$$

It includes the robot's position and orientation with respect to a fixed frame F_w, and the two components (with respect to the same frame) of the bias in GPS measurements.

After integrating the dynamic equations of the system through a standard Euler approximation with step size Δt=1, the system can be described with the following finite difference Equations:

$$\begin{cases} x_k = x_{k-1} + ds_{k-1} * \cos\theta_{k-1} \\ y_k = y_{k-1} + ds_{k-1} * \sin\theta_{k-1} \\ \theta_k = \theta_{k-1} + d\omega_{k-1} \\ x_{GPS,k} = x_{GPS,k-1} \\ y_{GPS,k} = y_{GPS,k-1} \end{cases} \quad with \quad \begin{matrix} ds = (dr + dl)/2 \\ d\omega = (dr - dl)/D \end{matrix} \quad (2)$$

The first three equations represent the discrete approximation of the robot's inverse kinematics, by assuming a unicycle differential drive model. As usual, *dr* and *dl* indicate the linear displacements of the right and left driving wheels, and D is the distance between them.

In the last two Equations, the dynamic of the bias $\mathbf{x}_{GPS}{}^T = \begin{bmatrix} x_{GPS} & y_{GPS} \end{bmatrix}$ is modeled. Notice that a constant dynamic is assumed for $\mathbf{x}_{GPS}{}^T$, since no cues are available to make more accurate hypotheses. This means that, when predicting the new state in the time-update phase of the EKF, $\mathbf{x}_{GPS}{}^T$ is left unchanged. However, the predicted value of $\mathbf{x}_{GPS}{}^T$ is updated whenever new measurement are available (i.e., in the correction phase of the EKF), thus finally producing an estimate that varies in time, and hopefully approximates the actual bias in GPS measurements. The approach seems reasonable whenever a component of the state vector changes slowly in time with respect to the remaining components, which is exactly the case.

When considering the remaining noise that affects **x**, the process can be described as governed by a non-linear stochastic difference Equation in the form

$$\mathbf{x}_k = \mathrm{f}(\mathbf{x}_{k-1}, \mathbf{u}_{k-1}, \mathbf{w}_{k-1}) \text{ with } \mathbf{x} \in \Re^5, \ \mathbf{w} = N(0, W) \quad (3)$$

where **w** represents the process noise, and **u** is the driving function; i.e., the 2-dimensional vector describing the current wheels displacements *dr* and *dl* ($\mathbf{u}^T = [dr \quad dl]$).

For what concerns errors in the process, they are currently modeled through a vector $\mathbf{w}^T = [wr \quad wl \quad wg]$. The first two element sums up to *dl* and *dr* (e.g., when the left encoder returns *dl*, the actual path traveled by the left wheel is *dl*+*wl*), whereas *wg* represents the error made in assuming that the bias has not changed since the last iteration of the Filter. By assuming that **w** has a zero-mean Gaussian distribution with covariance matrix **W**, systematic errors in odometry due to the approximate knowledge of the robot's geometric characteristics are not explicitly considered (in theory, geometric parameters should be included in the augmented state vector as well, as proposed in (Martinelli, 2002)).

Observations are provided both by the GPS and, when available, by the laser rangefinder. The measurements provided by the GPS are a non-linear function of the state:

$$\begin{cases} z_{long} = C_{LONG}(z_{lat}) * (x + x_{GPS}) \\ z_{lat} = C_{LAT}(z_{lat}) * (y + y_{GPS}) \end{cases} \quad (4)$$

Where $\mathbf{z}=(z_{long}, z_{lat})$ is a 2-dimensional vector representing the longitude and latitude of the mobile robot, by supposing the X-axis of F_w lying on the parallel passing through F_w's origin, and F_w's Y-axis lying on the meridian. The measurement model is not linear, mainly because the relationship between georeferenced data (i.e., latitude and longitude) and the estimated *x*- and *y*- coordinates varies with the latitude itself, as a consequence of the non planarity of the earth surface (as determined by $C_{LONG}(z_{lat})$ and $C_{LAT}(z_{lat})$).

For each line l_j observed by the laser rangefinder, the line m_i that best matches l_j can be expressed as:

$$\begin{cases} z_\rho = \dfrac{a_i \cdot x_k + b_i \cdot y_k + c_i}{\sqrt{a_i^2 + b_i^2}} \\ z_\alpha = \tan^{-1}\left(\dfrac{-a_i}{b_i}\right) - \theta_k \end{cases} \quad (5)$$

where a_i, b_i and c_i are the parameters characterizing the implicit equation of m_i; z_ρ and z_α are, respectively, the distance between the line and the robot, and the angle between the line and the robot's heading.

When putting together Equations 4 and 5, the measurement model results to be a non-linear function of the state:

$$\mathbf{z}_k = h(\mathbf{x}_k, \mathbf{v}_k) \qquad with \qquad \mathbf{v} = N(0, R) \quad (6)$$

Since non-AWG components of the GPS noise are estimated in the state vector, the remaining noise can be reasonably modeled with the vector **v**, a zero-mean AWG noise with covariance matrix **R.**

Equation 2 can be used to compute the a-priori state estimate at time *k*. Next, whenever new GPS or laser rangefinder data are available, they are fused with the a-priori estimate through an Extended Kalman Filter to produce a new estimate, thus reducing errors that are inherently present in odometry and providing a new estimate for the GPS bias.

Obviously, to evaluate the soundness of the previous assertion, it is necessary to perform an observability analysis of the system. The Kalman theorem requires to compute the observability matrix $Q = \left[H^T \mid A^T H^T \mid \ldots \mid (A^4)^T H^T\right]$, where *A* and *H* are the Jacobian matrices of the partial derivatives of *f* and *h* with respect to **x** (*Q*'s full expression is not shown for sake of brevity). The analysis shows that *Q* has full rank (and hence the state is fully observable) only when at least two observations l_j and l_m are available, corresponding to non-parallel lines m_i and m_n, together with a single GPS measurement.

Matrix *A* results to be:

$$A = \begin{bmatrix} 1 & 0 & -ds_{k-1} \cdot \sin(\theta_{k-1}) & 0 & 0 \\ 0 & 1 & ds_{k-1} \cdot \cos(\theta_{k-1}) & 0 & 0 \\ 0 & 0 & 1 & 0 & 0 \\ 0 & 0 & 0 & 1 & 0 \\ 0 & 0 & 0 & 0 & 1 \end{bmatrix} \quad (7)$$

whereas *H* results to be:

$$H = \begin{bmatrix} 1/C_{LONG} & 0 & 0 & 1/C_{LONG} & 0 \\ 0 & 1/C_{LAT} & 0 & 0 & 1/C_{LAT} \\ \dfrac{a_i}{\sqrt{a_i^2 + b_i^2}} & \dfrac{b_i}{\sqrt{a_i^2 + b_i^2}} & 0 & 0 & 0 \\ 0 & 0 & -1 & 0 & 0 \\ \dfrac{a_m}{\sqrt{a_m^2 + b_m^2}} & \dfrac{b_m}{\sqrt{a_m^2 + b_m^2}} & 0 & 0 & 0 \\ 0 & 0 & -1 & 0 & 0 \end{bmatrix} \quad (8)$$

By inspecting matrix *H*, one could infer that the filter is updated only when a triplet of observations are available (i.e., two non-parallel lines and one

GPS measurement). However, this is assumed only to investigate the state's observability; during experiments, the laser rangefinder and the GPS returns observations asynchronously, and each observation is used to update the state as soon as available. The observability analysis demonstrates that, even if each measurement is able to correct the state only partially, the state is fully observable when more measurements are considered in cascade.

Unfortunately, in outdoor areas it often happens that the laser cannot detect any line mapped in the a-priori map: since the localization algorithm relies only on GPS data, the H matrix fed to the KF comprises only the first two rows in Equation 8. When this happens – as already stated - only a subspace of the state space results to be observable; by computing again the observability matrix Q, this yields the result in Equation 9.

When $ds_{k-1} \neq 0$, i.e. when the translational speed of the robot is not null (Capezio, *et al.*, 2005), the rank of Q is 3. The rank is not full since Q's first column (corresponding to the x-component of the state vector **x**) equals the fourth column (corresponding to the x_{GPS}-component), and Q's second column (i.e., the y-component) equals the fifth column (i.e., the y_{GPS}-component). On the opposite, Q's third column (corresponding to the θ-component of **x**) is linearly independent from the others.

Q's analysis confirms the intuition that – when no laser data are available – the subspace defined by $x+x_{GPS}$, $y+y_{GPS}$, and θ is fully observable: the robot's orientation is still corrected by GPS data (when $ds_{k-1} \neq 0$, see also (Capezio, *et al.*, 2005)), and the position has a permanent error that depends on the current estimate of the GPS bias.

$$Q = \begin{bmatrix} 1/C_{LONG} & 0 & 0 & 1/C_{LONG} & 0 \\ 0 & 1/C_{LAT} & 0 & 0 & 1/C_{LAT} \\ 1/C_{LONG} & 0 & -\frac{1}{C_{LONG}} \cdot ds_{k-1} \cdot \sin(\theta_{k-1}) & 1/C_{LONG} & 0 \\ 0 & 1/C_{LAT} & \frac{1}{C_{LAT}} \cdot ds_{k-1} \cdot \cos(\theta_{k-1}) & 0 & 1/C_{LAT} \\ 1/C_{LONG} & 0 & -\frac{2}{C_{LONG}} \cdot ds_{k-1} \cdot \sin(\theta_{k-1}) & 1/C_{LONG} & 0 \\ 0 & 1/C_{LAT} & \frac{2}{C_{LAT}} \cdot ds_{k-1} \cdot \cos(\theta_{k-1}) & 0 & 1/C_{LAT} \\ 1/C_{LONG} & 0 & -\frac{3}{C_{LONG}} \cdot ds_{k-1} \cdot \sin(\theta_{k-1}) & 1/C_{LONG} & 0 \\ 0 & 1/C_{LAT} & \frac{3}{C_{LAT}} \cdot ds_{k-1} \cdot \cos(\theta_{k-1}) & 0 & 1/C_{LAT} \\ 1/C_{LONG} & 0 & -\frac{4}{C_{LONG}} \cdot ds_{k-1} \cdot \sin(\theta_{k-1}) & 1/C_{LONG} & 0 \\ 0 & 1/C_{LAT} & \frac{4}{C_{LAT}} \cdot ds_{k-1} \cdot \cos(\theta_{k-1}) & 0 & 1/C_{LAT} \end{bmatrix} \quad (9)$$

In this case, the innovation due to GPS measurements is distributed by the Kalman gain onto x-, y-, x_{GPS}, and y_{GPS} components of the state according to the current value of the state covariance matrix **P**. Since a constant dynamic is assumed for x_{GPS}, and y_{GPS}, corrections are adequately distributed onto the state components only if the actual bias in GPS changes slowly, and given that a new area where the laser rangefinder is able to guarantee full observablility will soon be available. This is reasonable when assuming a cyclic patrol path for autonomous surveillance, with periodic visits to outdoor areas that are mapped in the a-priori model and observable by the laser.

4 EXPERIMENTAL RESULTS

Many experiments in a realistic simulated environment and at the Albenga Airport (Figure 6) have been performed. Moreover, in order to test the system under different conditions, experiments are performed by varying the robot' speed. The GPS sensor is realistically simulated (data are taken from real GPS in a 24-hours interval), as well as errors in laser measurements and odometry.

In all the simulated tests, the robot is requested to move along a path that is identical to the patrol performed in Villanova d'Albenga Airport. Furthermore, the dimension and the position of the exterior walls of buildings considered for map-based localization in the simulated environment realistically emulate the Airport scenario (see Figure 3; walls are visible only in a very limited area of the Airport). The simulated robot travels for the whole day, performing a cyclic patrol about 500 meters long; next, the experiment is repeated by varying the navigation speed.

Tests have been performed in two modalities: A-tests correspond to localization with GPS bias estimation, and B-tests are performed without bias estimation.

Table 1: Errors statistics in B-tests.

Nav. Speed (m/s).	$\bar{e}_x$	σ_x	$\bar{e}_y$	σ_y	$\bar{e}_\vartheta$	σ_ϑ
0.4	1.50	1.01	1.18	0.55	0.067	0.047
0.9	1.36	0.97	1.75	1.22	0.048	0.039
1.4	1.47	1.14	1.29	0.72	0.043	0.035

Table 2: Errors statistics in A-test.

Nav. Speed (m/s).	$\bar{e}_x$	σ_x	$\bar{e}_y$	σ_y	$\bar{e}_\vartheta$	σ_ϑ
0.4	1.07	1.04	1.63	1.13	0.057	0.053
0.9	0.94	0.84	0.78	0.70	0.040	0.033
1.4	0.97	0.80	1.23	1.14	0.041	0.031

Tables 1 and 2 summarize results. In Table 1, results of the B-tests are shown. In this case the state vector includes only the position and the orientation of the robot. Table 2 shows the results of A-tests. In both Tables, $\bar{e}_x$ and $\bar{e}_y$ represent the average error between *x*- and *y*- components of **x** and the real robot's position (ground truth); $\bar{e}_\vartheta$ is the average error in the robot's heading; σ_x, σ_y, σ_ϑ are the corresponding standard deviations.

When computing the average position error as $\mathbf{x}_{err} = E(\sqrt{e_x^2 + e_y^2})$, this yields:

- B-tests: $\mathbf{x}_{err}$=2.12m, $\mathbf{x}_{err}$=1.92m, and $\mathbf{x}_{err}$=2.08m when the robot is moving at the speed of 0.4m/s, 0.9m/s, and 1.4m/s respectively
- A-tests: $\mathbf{x}_{err}$=1.52m,$\mathbf{x}_{err}$ =1.34m, and $\mathbf{x}_{err}$ =1.37m (for 0.4m/s, 0.9m/s, and 1.4m/s).

By analyzing the data, some considerations can be made:

- $\mathbf{x}_{err}$ is always below 2.5m, with and without the GPS bias Estimation.
- In the best case (1.4m/sec navigation speed), the bias estimation reduces $\mathbf{x}_{err}$ of about 34%.
- The improvement due to GPS bias estimation seems to increase when the navigation speed increase; this could be consequence of the fact that the robot returns quicker in areas where laser-based localization is possible.
- Standard deviations are always comparable with averages; i.e., the error oscillates significantly around its mean value.
- Errors in the θ-component are bounded, and always below 10 degrees.

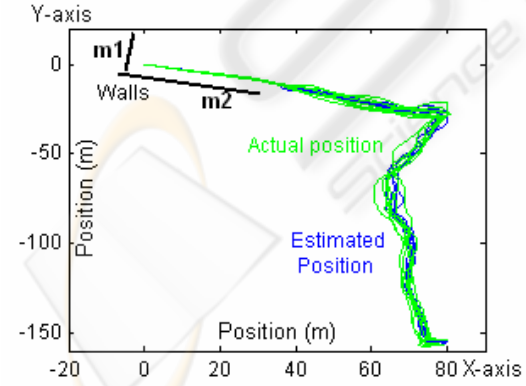

Figure 3: Test performed at 0.9 m/sec.

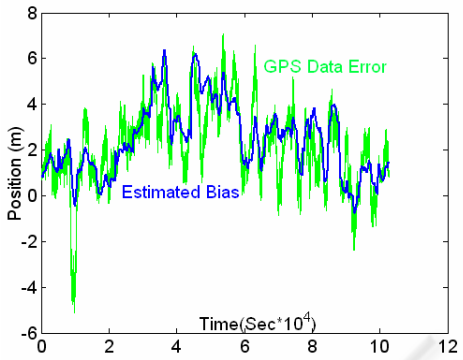

Figure 4: GPS bias estimation.

Figure 3 shows a plot of the robot's trajectory during an A-test 3 hours long (moving at 0.9 m/sec); Figure 4 shows the estimated longitude bias during such test

Real world experiments have been carried out as well with the ANSER robot in the Albenga Airport. During the test, the robot is manually driven at 1.0m/s along a pre-established cyclic path that is about 500 meters long (walls are similar to Figure 3). Different A- and B-tests are been performed (each lasting about 3 hours), by memorizing the robot's estimated position in a finite number of selected places along the path.

Figure 5 shows the estimated robot's position in 8 different places along the real path (the Figure can be superimposed onto Figure 3 to infer where features for laser-based localization are visible).

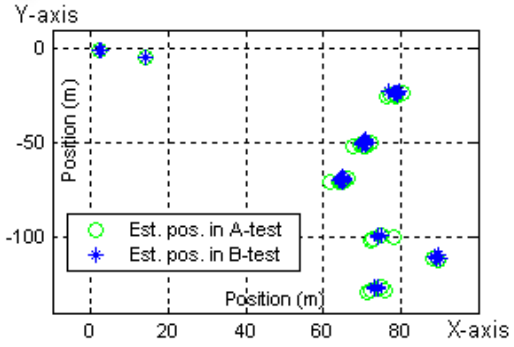

Figure 5: Estimated position in a real scenario.

In the real scenario, A-tests exhibit a smaller improvement in performance with respect to simulation. This is probably due to the fact that the state is fully observable (and hence the GPS bias can be correctly estimated) only when laser data are available. However, this happens in the vicinity of buildings (e.g., walls in Figure 3 correspond to a hangar); unfortunately, near a building the GPS

signal is less precise, since the GPS satellites are occluded by the building itself.

Figure 6: The robot ANSER at Albenga Airport.

5 CONCLUSIONS

The paper describes the localization subsystem of a mobile robot that has been designed for night patrols and surveillance tasks within a civilian airport. The localization subsystem is a small – but fundamental component – of the whole project (ANSER – Airport Night Surveillance Expert Robot). Instead of equipping the robot with a huge amount of expensive sensors (and the computing power that is adequate to deal with them), a simple approach is chosen that relies exclusively on a non-differential GPS unit and a laser rangefinder (i.e., inertial sensors are absent). Laser measurements are exploited only in some areas of the outdoor patrol path of the robot, i.e. where it is possible detect line features and match them against an a-priori model of the environment. Along the rest of the path, the robot relies on GPS-based localization. An Extended Kalman Filter algorithm is employed to estimate an augmented state vector comprising the robot position and orientation, together with the low frequency components (bias) of the GPS error.

A formal model of the whole localization subsystem is given, including an analysis of the system's observability. The experiments performed in a realistic simulated environment and at Villanova d'Albenga Airport have confirmed the expectations, showing that the approach reasonably improves the localization accuracy of the system. Obviously, the accuracy achieved is not sufficient for fine motion in cluttered areas; however, for surveillance applications in which the robot has to reach an area of interest and to further investigate on the basis of local sensor feedback, it seems appropriate.

REFERENCES

Capezio, F., Sgorbissa, A., and Zaccaria (2005), R. GPS-based Localizzation for UGV Performing Surveillance Patrols in Wide Outdoor Areas, In *proc. of Int. Conf. on Field and Service Robotics*,

Capezio, F., Mastrogiovanni, F., Sgorbissa, A., and Zaccaria, R. (2006), Fast Position Tracking of an Autonomous Vehicle in Cluttered and Dynamic Indoor Environments, In *proc. of 8th International IFAC Symposium on Robot Control*

Dissanayake, G., Sukkarieh, S., Nebot, E. and Durrant-Whyte, H. (2001), The aiding of a low-cost strapdown inertial measurement unit using vehicle model constraints for land vehicle applications, In *IEEE Trans. on Robotics and Automation*, vol. 17, Issue 5, pp. 731 – 747,

Farrell, J. A., Givargis, T. and Barth, M. (2000), Real-time differential carrier phase GPS-aided INS, In *IEEE Trans. Contr. Syst. Technol*., vol. 8, pp. 709-721.

Heath-Pastore, T., H.R. Everett, and K. Bonner (1999), Mobile Robots for Outdoor Security Applications, In *American Nuclear Society 8th International Topical Meeting on Robotics and Remote Systems*, Pittsburgh.

Martinelli, A. (2002) The Odometry Error of a Mobile Robot with a Synchronous Drive System. In *IEEE Trans. on Robotics and Automation*, Vol 18, no. 3, pp 399-405.

Panzieri, S., Pascucci, F., and Ulivi, G. (2002), An Outdoor Navigation System Using GPS and Inertial Platform, I*EEE Trans. on mechatronics*, vol. 7, no 2

Rybski, P. E., Stoeter, S. A., Gini, M., Hougen, D. F. and Papanikolopoulos, N P. (2002), Performance of a Distributed Robotic System Using Shared Communications Channels, In *IEEE Trans on Robotics and Automation*, vol. 18, no.5

Saptharishi M., Oliver, C. S., Diehl, C. P., Bhat, K. S., Dolan, J. M., Trebi-Ollennu, A. and Khosla, P. K. (2002), Distributed Surveillance and Reconnaissance Using Multiple Autonomous ATVs: CyberScout, In *IEEE Trans. on Robotics and Automation,* vol. 18, no.5

Sasiadek, J. Z. and Wang, Q. (2003), Low cost automation using INS/GPS data fusion for accurate positioning, In *Robotica,* Vol. 21, pp. 255-260. Cambridge University Press.

Schönberg, T., Ojala, M., Suomela, J., Torpo, A., and Halme, A (1995), Positioning an autonomous off-road vehicle by using fused DGPS and inertial navigation, In *2nd IFAC Conference on Intelligent Autonomous Vehicles*, Espoo, pp. 226-231

Vidal, R.,, Shakernia, O., Kim, H. j., Shim, D. H. and, Sastry, S. (2002), Probabilistic Pursuit–Evasion Games: Theory, Implementation, and Experimental Evaluation, In *IEEE Trans. on Robotics and Automation*, vol. 18, no. 5,

Volkan, I., Sampath, K. and Sanjeev K. (2005), Randomized Pursuit-Evasion in a Polygonal Environment, In *IEEE Trans. on robotics*,vol.21, no. 5